



Match-up database Analyses Report

Aquarius-L3-JPL-V4-7DAY-RUNNING

Sea mammals

Indian Ocean

prepared by the Pi-MEP Consortium

May 15, 2018

Contents

1	Overview	3
2	The MDB file datasets	4
2.1	Satellite SSS product	4
2.1.1	Aquarius-L3-JPL-V4-7DAY-RUNNING	4
2.2	In situ SSS dataset	4
2.3	Auxiliary geophysical datasets	5
2.3.1	CMORPH	5
2.3.2	ASCAT	6
2.3.3	ISAS	6
2.3.4	World Ocean Atlas Climatology	7
2.4	Overview of the Match-ups generation method	7
2.4.1	In Situ/Satellite data filtering	7
2.4.2	In Situ/Satellite Co-localization	8
2.4.3	MDB pair Co-localization with auxiliary data and complementary information	8
2.4.4	Content of the Match-Up NetCDF files	9
2.5	MDB characteristics for the particular in situ/satellite pairs	14
2.5.1	Number of paired SSS data as a function of time and distance to coast	14
2.5.2	Histograms of the SSS match-ups	14
2.5.3	Distribution in situ SSS depth in match-ups pairs	15
2.5.4	Spatial Distribution of Match-ups	15
2.5.5	Histograms of the spatial and temporal lags of the match-ups pairs	16
3	MDB file Analyses	16
3.1	Spatial Maps of the Temporal mean and STD of in situ and satellite SSS and of the difference (Δ SSS)	16
3.2	Time series of the monthly averaged mean and STD of in situ and satellite SSS and of the (Δ SSS)	17
3.3	Zonally-averaged Time-mean and temporal STD of in situ and satellite SSS and of the Δ SSS	18
3.4	Scatterplots of satellite vs in situ SSS by latitudinal bands	20
3.5	Time series of the monthly averaged mean and STD of the Δ SSS sorted by latitudinal bands	21
3.6	Δ SSS sorted as function of geophysical conditions	21
4	Summary	24

Acronym

Aquarius	NASA/CONAE Salinity mission
ASCAT	Advanced Scatterometer
ATBD	Algorithm Theoretical Baseline Document
BLT	Barrier Layer Thickness
CMORPH	CPC MORPHing technique
CTD	Instrument used to measure the conductivity, temperature, and pressure of seawater
DM	Delayed Mode
EO	Earth Observation
ESA	European Space Agency
FTP	File Transfer Protocol
GOSUD	Global Ocean Surface Underway Data
GT MBA	The Global Tropical Moored Buoy Array
Ifremer	Institut français de recherche pour l'exploitation de la mer
IPEV	Institut polaire français Paul-Émile Victor
IQR	Interquartile range
ISAS	In Situ Analysis System
L2	Level 2
LEGOS	Laboratoire d'Etudes en Géophysique et Océanographie Spatiales
LOCEAN	Laboratoire d'Océanographie et du Climat : Expérimentations et Approches Numériques
LOPS	Laboratoire d'Océanographie Physique et Spatiale
MDB	Match-up database
MEOP	Marine Mammals Exploring the Oceans Pole to Pole
MLD	Mixed Layer Depth
NRT	Near Real Time
Pi-MEP	Pilot Mission Exploitation Platform
PIRATA	Prediction and Researched Moored Array in the Atlantic
QC	Quality control
R_{sat}	Spatial resolution of the satellite SSS product
RAMA	Research Moored Array for African-Asian-Australian Monsoon Analysis and Prediction
RR	Rain rate
SAMOS	Shipboard Automated Meteorological and Oceanographic System
SMAP	Soil Moisture Active Passive (NASA mission)
SMOS	Soil Moisture and Ocean Salinity (ESA mission)
SSS	Sea Surface Salinity
$SSS_{in situ}$	In situ SSS data considered for the match-up
SSS_{SAT}	Satellite SSS product considered for the match-up
ΔSSS	Difference between satellite and in situ SSS at colocalized point ($\Delta SSS = SSS_{SAT} - SSS_{in situ}$)
SST	Sea Surface Temperature
STD	Standard deviation
Survostral	SURVeillance de l'Océan AuSTRAL (Monitoring the Southern Ocean)
TAO	Tropical Atmosphere Ocean
TSG	Thermosalinograph

1 Overview

In this report, we present systematic analyses of the Match-up DataBase (MDB) files generated by the Pi-MEP platform within the following Pi-MEP region and for the below pair of Satellite/In situ SSS data:

- Pi-MEP region: Indian Ocean
- SSS satellite product (SSS_{SAT}): Aquarius-L3-JPL-V4-7DAY-RUNNING
- In situ dataset ($SSS_{In situ}$): Sea mammals

In the following, $\Delta SSS = SSS_{SAT} - SSS_{In situ}$ denotes the difference between the satellite and in situ SSS at the colocalized points that form the MDB.

This report presents successively:

The MDB file DataSets (Section 2)

- A short description of the satellite SSS product considered in the match-up (2.1)
- A short description of the In situ SSS dataset considered in the match-up (2.2)
- A short description of the auxiliary geophysical datasets co-localized with SSS pairs (2.3)
- An overview of how the Match-ups were evaluated (2.4)
- An overview of the MDB characteristics for the particular in situ/satellite pairs (2.5)

The major results of the MDB file Analyses (Section 3)

- Spatial Maps of the Time-mean and temporal STD of in situ and satellite SSS and of the ΔSSS (3.1)
- Time series of the monthly averaged mean and STD of in situ and satellite SSS and of the ΔSSS (3.2)
- Zonally-averaged Time-mean and temporal STD of in situ and satellite SSS and of the ΔSSS (3.3)
- Scatterplots of satellite vs in situ SSS by latitudinal bands (3.4)
- Time series of the monthly averaged mean and STD of the ΔSSS sorted by latitudinal bands (3.5)
- ΔSSS sorted as function of geophysical conditions (3.6)

All analyses are conducted over the Pi-MEP Region specified above and over the full satellite SSS product period.

2 The MDB file datasets

2.1 Satellite SSS product

2.1.1 Aquarius-L3-JPL-V4-7DAY-RUNNING

Version 4.0 Aquarius CAP Level 3 products are the third release of the AQUARIUS/SAC-D mapped salinity and wind speed data based on the Combined Active Passive (CAP) algorithm. Level 3 standard mapped image products contain gridded 1 degree spatial resolution salinity and wind speed data averaged over 7 day and monthly time scales. This particular data set is the 7-Day running mean sea surface salinity (SSS) V4.0 Aquarius CAP product. CAP is a P.I. produced data set developed and provided by the JPL Climate Oceans and Solid Earth group (S. Yueh). The CAP algorithm utilizes data from both the onboard radiometer and scatterometer to simultaneously retrieve salinity, wind speed and direction by minimizing the sum of squared differences between model and observations. The main improvement in CAP V4.0 is calibration of the rain roughness correction geophysical model function to HYCOM SSS adjusted by the Rain Impact Model (RIM) to account for the rain induced near surface stratification. Rain corrected salinity retrieval at L2 is based on collocation with ancillary rain rate from NOAA CMORPH at 0.25 degree and 30 minute resolution, replacing the SSMI/S and WindSAT data previously used previously for this in CAP V3.0. The Aquarius instrument is onboard the AQUARIUS/SAC-D satellite, a collaborative effort between NASA and the Argentinian Space Agency Comision Nacional de Actividades Espaciales (CONAE). The instrument consists of three radiometers in push broom alignment at incidence angles of 29, 38, and 46 degrees incidence angles relative to the shadow side of the orbit. Footprints for the beams are: 76 km (along-track) x 94 km (cross-track), 84 km x 120 km and 96km x 156 km, yielding a total cross-track swath of 370 km. The radiometers measure brightness temperature at 1.413 GHz in their respective horizontal and vertical polarizations (TH and TV). A scatterometer operating at 1.26 GHz measures ocean backscatter in each footprint that is used for surface roughness corrections in the estimation of salinity. The scatterometer has an approximate 390km swath.

Table 1: Satellite SSS product characteristics

Aquarius-L3-JPL-V4-7DAY-RUNNING	
Spatial resolution	1°x1°
Temporal repeat	7 Day
Temporal coverage	From 2011-08-25 to 2015-06-07
Spatial coverage	Global [-180 180 -90 90]
Data Provider	Simon Yueh at Jet Propulsion Laboratory, Pasadena, USA
Release Date	2015-10-07
Version	4
User Guide	Aquarius-CAP-User-Guide-v4.0.pdf
Documentation	ftp://podaac-ftp.jpl.nasa.gov/allData/aquarius/docs/CAPv4/
DOI	http://dx.doi.org/10.5067/AQR40-3T7CS

2.2 In situ SSS dataset

Instrumentation of southern elephant seals with satellite-linked CTD tags proposes unique temporal and spatial coverage. This includes extensive data from the Antarctic continental slope

and shelf regions during the winter months, which is outside the conventional areas of Argo autonomous floats and ship-based studies. The use of elephant seals has been particularly effective to sample the Southern Ocean and the North Pacific. Other seal species have been successfully used in the North Atlantic, such as hooded seals. The marine mammal dataset ([MEOP-CTD database](#)) is quality controlled and calibrated using delayed-mode techniques involving comparisons with other existing profiles as well as cross-comparisons similar to established protocols within the Argo community, with a resulting accuracy of ± 0.03 °C in temperature and ± 0.05 in salinity or better ([Treasure et al. \(2017\)](#)). It is available www.seanoe.org and is updated once a year. The marine mammal data were collected and made freely available by the International MEOP Consortium and the national programs that contribute to it. (<http://www.meop.net>). A preprocessing stage is applied to the database before being used by the Pi-MEP which consist to keep only profile with salinity, temperature and pressure quality flags set to 1 or 2 and a profile is kept if at least one measurement is in the top 10 m depth. Marine mammal SSS correspond to the top (shallowest) profile salinity data provided that profile depth is 10 m or less.

2.3 Auxiliary geophysical datasets

Additional EO datasets are used to characterize the geophysical conditions at the in situ/satellite SSS pair measurement locations and time, and 10 days prior the measurements to get an estimate of the geophysical condition and history. As discussed in [Boutin et al. \(2016\)](#), the presence of vertical gradients in, and horizontal variability of, sea surface salinity indeed complicates comparison of satellite and in situ measurements. The additional EO data are used here to get a first estimates of conditions for which L-band satellite SSS measured in the first centimeters of the upper ocean within a 50-150 km diameter footprint might differ from pointwise in situ measurements performed in general between 10 and 5 m depth below the surface. The spatio-temporal variability of SSS within a satellite footprint (50–150 km) is a major issue for satellite SSS validation in the vicinity of river plumes, frontal zones, and significant precipitation. Rainfall can in some cases produce vertical salinity gradients exceeding 1 pss m^{-1} ; consequently, it is recommended that satellite and in situ SSS measurements less than 3–6 h after rain events should be considered with care when used in satellite calibration/validation analyses. To identify such situation, the Pi-MEP test platform is first using [CMORPH](#) products to characterize the local value and history of rain rate and [ASCAT](#) gridded data are used to characterize the local surface wind speed and history.

2.3.1 CMORPH

Precipitation are estimated using the [CMORPH](#) 3-hourly products at $1/4^\circ$ resolution ([Joyce et al. \(2004\)](#)). CMORPH (CPC MORPHing technique) produces global precipitation analyses at very high spatial and temporal resolution. This technique uses precipitation estimates that have been derived from low orbiter satellite microwave observations exclusively, and whose features are transported via spatial propagation information that is obtained entirely from geostationary satellite IR data. At present NOAA incorporate precipitation estimates derived from the passive microwaves aboard the DMSP 13, 14 and 15 (SSM/I), the NOAA-15, 16, 17 and 18 (AMSU-B), and AMSR-E and TMI aboard NASA's Aqua, TRMM and GPM spacecraft, respectively. These estimates are generated by algorithms of [Ferraro \(1997\)](#) for SSM/I, [Ferraro et al. \(2000\)](#) for AMSU-B and [Kummerow et al. \(2001\)](#) for TMI. Note that this technique is not a precipitation estimation algorithm but a means by which estimates from existing microwave rainfall algorithms can be combined. Therefore, this method is extremely flexible such that any precipitation estimates from any microwave satellite source can be incorporated.

With regard to spatial resolution, although the precipitation estimates are available on a grid with a spacing of 8 km (at the equator), the resolution of the individual satellite-derived estimates is coarser than that - more on the order of 12 x 15 km or so. The finer "resolution" is obtained via interpolation.

In effect, IR data are used as a means to transport the microwave-derived precipitation features during periods when microwave data are not available at a location. Propagation vector matrices are produced by computing spatial lag correlations on successive images of geostationary satellite IR which are then used to propagate the microwave derived precipitation estimates. This process governs the movement of the precipitation features only. At a given location, the shape and intensity of the precipitation features in the intervening half hour periods between microwave scans are determined by performing a time-weighting interpolation between microwave-derived features that have been propagated forward in time from the previous microwave observation and those that have been propagated backward in time from the following microwave scan. NOAA refer to this latter step as "morphing" of the features.

For the present Pi-MEP products, we only considered the 3-hourly products at 1/4 degree resolution. The entire CMORPH record (December 2002-present) for 3-hourly, 1/4 degree lat/lon resolution can be found at: ftp://ftp.cpc.ncep.noaa.gov/precip/CMORPH_V1.0/RAW/. CMORPH estimates cover a global belt (-180°W to 180°E) extending from 60°S to 60°N latitude and are available for the complete period of the Pi-MEP core datasets (Jan 2010-now).

2.3.2 ASCAT

Advanced SCATterometer (ASCAT) daily data produced and made available at Ifremer/CERSAT on a 0.25°x0.25° resolution grid (Bentamy and Fillon (2012)) since November 2008 are used to characterize the mean daily wind at the match-up pair location as well as the wind history during the 10-days period preceding the in situ measurement date. These wind fields are calculated based on a geostatistical method with external drift. Remotely sensed data from ASCAT are considered as observations while those from numerical model analysis (ECMWF) are associated with the external drift. The spatial and temporal structure functions for wind speed, zonal and meridional wind components are estimated from ASCAT retrievals. Furthermore, the new procedure includes a temporal interpolation of the retrievals based on the complex empirical orthogonal function (CEOF) approach, in order to enhance the sampling length of the scatterometer observations. The resulting daily wind fields involves the main known surface wind patterns as well as some variation modes associated with temporal and spatial moving features. The accuracy of the gridded winds was investigated through comparisons with moored buoy data in Bentamy et al. (2012) and resulted in rms differences for wind speed and direction are about 1.50 m.s⁻¹ and 20°.

2.3.3 ISAS

The In Situ Analysis System (ISAS), as described in Gaillard et al. (2016) is a data based re-analysis of temperature and salinity fields over the global ocean. It was initially designed to synthesize the temperature and salinity profiles collected by the ARGO program. It has been later extended to accommodate all type of vertical profile as well as time series. ISAS gridded fields are entirely based on in-situ measurements. The methodology and configuration have been conceived to preserve as much as possible the data information content and resolution. ISAS is developed and run in a research laboratory (LOPS) in close collaboration with Coriolis, one of ARGO Global Data Assembly Center and unique data provider for the Mercator operational oceanography system. At the moment the period covered starts in 2002 and only the upper 2000m are considered. The gridded fields were produced over the global ocean 70°N–70°S on

a $1/2^\circ$ grid by the ISAS project with datasets downloaded from the Coriolis data center (for more details on ISAS see Gaillard et al. (2009)). In the PiMEP, the product in used is the [INSITU_GLO_TS_OA_NRT_OBSERVATIONS_013_002_a](#) v6.2 NRT derived at the Coriolis data center and provided by Copernicus (www.marine.copernicus.eu/documents/PUM/CMEMS-INS-PUM-013-002-ab.pdf). The major contribution to the data set is from Argo array of profiling floats, reaching an approximate resolution of one profile every 10-days and every 3-degrees over the Satellite SSS period (<http://www.umar-lops.fr/SNO-Argo/Products/ISAS-T-S-fields/>); in this version SSS from thermosalinographs from ship of opportunity are not used, so that we can consider SMOS SSS validation using ship of opportunity measurements independent of ISAS. The ISAS optimal interpolation involves a structure function modeled as the sum of two Gaussian functions, each associated with specific time and space scales, resulting in a smoothing over typically 3 degrees. The smallest scale which can be retrieved with ISAS analysis is not smaller than 300–500 km (Kolodziejczyk et al. (2015)). For validation purpose, the ISAS monthly SSS fields at depth level 5 m are collocated and compared with the satellite SSS products and included in the PiMEP MDB files. In addition, the « percentage of variance » fields (PCTVAR) contained in the ISAS analyses provide information on the local variability of in situ SSS measurements within $1/2^\circ \times 1/2^\circ$ boxes.

2.3.4 World Ocean Atlas Climatology

The World Ocean Atlas 2013 version 2 ([WOA13 V2](#)) is a set of objectively analyzed (1° grid) climatological fields of in situ temperature, salinity and other variables provided at standard depth levels for annual, seasonal, and monthly compositing periods for the World Ocean. It also includes associated statistical fields of observed oceanographic profile data interpolated to standard depth levels on 5° , 1° , and 0.25° grids. We use these fields in complement to ISAS to characterize the climatological fields (monthly mean and std) at the match-up pairs location and date.

2.4 Overview of the Match-ups generation method

The match-up production is basically a three steps process:

1. preparation of the input in situ and satellite data, and,
2. co-localization of satellite products with in situ SSS measurements.
3. co-localization of the in situ/satellite pair with auxiliary information.

In the following, we successively detail the approaches taken for these different steps.

2.4.1 In Situ/Satellite data filtering

The first step consist in filtering Sea mammals in situ dataset using the quality flags as described in 2.2 so that only valid salinity data remains in the produced match-ups.

For high-spatial resolution in situ SSS measurements such as the Thermo-SalinoGraph (TSG) SSS data from research vessels, Voluntary Observing Ships (VOS) or sailing ships, as well as SSS data from surface drifters, an additional spatial-filtering step is performed on the in situ data that will be in fine compared to the satellite SSS products. If R_{sat} is the spatial resolution of the satellite SSS product (L2 to L3-L4), we keep the in situ data at the original spatial resolution but we also estimate for all spatio-temporal samples a running median filtered SSS applied to all neighbouring in situ SSS data acquired within a distance of $R_{sat}/2$ from a given in situ acquisition. Both the original and the filtered data are finally stored in the MDB files.

Only for satellite L2 SSS data, a third step consist in filtering spurious data using the flags and associated recommendation as provided by the official data centers and described in 2.1.

2.4.2 In Situ/Satellite Co-localization

In this step, each SSS satellite acquisition is co-localized with the filtered in situ measurements. The method used for co-localization differ if the satellite SSS is a swath product (so-called Level 2-types) or a time-space composite product (so-called Level 3/level 4-types).

- For L2 SSS swath data :

If R_{sat} is the spatial resolution of the satellite swath SSS product, for each in situ data sample collected in the Pi-MEP database, the platform searches for all satellite SSS data found at grid nodes located within a radius of $R_{sat}/2$ from the in situ data location and acquired with a time-lag from the in situ measurement date that is less or equal than ± 6 hours. If several satellite SSS samples are found to meet these criteria, the final satellite SSS match-up point is selected to be the closest in time from the in situ data measurement date. The final spatial and temporal lags between the in situ and satellite data are stored in the MDB files.

- For L3 and L4 composite SSS products :

If R_{sat} is the spatial resolution of the composite satellite SSS product and D the period over which the composite product was built (e.g., periods of 1, 7, 8, 9, 10, 18 days, 1 month, etc..) with central time t_0 , for each in situ data sample collected in the Pi-MEP database during period D, the platform searches for all satellite SSS data of the composite product found at grid nodes located within a radius of $R_{sat}/2$ from the in situ data location. If several satellite SSS product samples are found to meet these criteria, the final satellite SSS match-up point is chosen to be the composite SSS with central time t_0 which is the closest in time from the in situ data measurement date. The final spatial and temporal lags between the in situ and satellite data are stored in the MDB files.

2.4.3 MDB pair Co-localization with auxiliary data and complementary information

MDB data consist of satellite and in-situ SSS pair datasets but also of auxiliary geophysical parameters such as local and history of wind speed and rain rates, as well as various information (climatology, distance to coast, mixed layer depth, barrier layer thickness, etc) that can be derived from in situ data and which are included in the final match-up files. The collocation of auxiliary parameters and additional information is done for each filtered in-situ SSS measurement contained in the match-up files as follows :

If t_{insitu} is the time/date at which the in situ measurement is performed, we collect:

- The [ASCAT](#) wind speed product of the same day than t_{insitu} found at the ASCAT $1/4^\circ$ grid node with closest distance from the in situ data location and the time series of the ASCAT wind speed at the same node for the 10 days prior the in situ measurement day.
- If the in situ data is located within the 60°N - 60°S band, we select the [CMORPH](#) 3-hourly product the closest in time from t_{insitu} and found at the CMORPH $1/4^\circ$ grid node with closest distance from the in situ data location. We then store the time series of the CMORPH rain rate at the same node for the 10 days prior the in situ measurement time.

For the given month/year of the in situ data, we select the [ISAS](#) and [WOA](#) fields for the same month (and same year for ISAS fields) and take the SSS analysis (monthly mean, std) found at the grid node the closest from the in situ measurement.

The distance from the in situ SSS data location to the nearest coast is evaluated and provided in kms. We use a distance-to-coast map derived by CLS with a spatial resolution of $1/16^\circ$ that we re-gridded at $1/4^\circ$ resolution taking the minimum value of all $1/16^\circ$ observations found in the $1/4^\circ$ grid cell.

When vertical profiles of S and T are made available from the in situ measurements used to build the match-up (Argo or sea mammals), the following variables are included into each satellite/in situ match-up file:

1. The vertical distribution of pressure at which the profile were measured,
2. The vertical $S(z)$ and $T(z)$ profiles,
3. The vertical potential density anomaly profile $\sigma_0(z)$,
4. The Mixed Layer Depth (MLD). The MLD is defined here as the depth where the potential density has increased from the reference depth (10 meter) by a threshold equivalent to 0.2°C decrease in temperature at constant salinity: $\sigma_0 = \sigma_{010m} + \Delta\sigma_0$ with $\Delta\sigma_0 = \sigma_0(\theta_{10m} - 0.2, S_{10m}) - \sigma_0(\theta_{10m}, S_{10m})$ where θ_{10m} and S_{10m} are the temperature and salinity at the reference depth (i.e. 10 m) ([de Boyer Montégut et al. \(2004\)](#), [de Boyer Montégut et al. \(2007\)](#)).
5. The Top of the Thermocline Depth (TTD) is defined as the depth at which temperature decreases from its 10 m value by 0.2°C .
6. The Barrier Layer if present, is defined as the intermediate layer between the top of the thermocline and the bottom of the density mixed-layer and its thickness (BLT) is defined as the difference between the MLD and the TTD.
7. The vertical profile of the buoyancy frequency $N^2(z)$

The resulting match-ups files are serialized as NetCDF-4 files whose structure depends on the origin of the in-situ data they contain.

2.4.4 Content of the Match-Up NetCDF files

```
netcdf pimep-mdb-aquarius-l3-jpl-v4-7dr_seal_20100116_v01 {
dimensions:
N_prof = 1 ;
N_LEVELS = 27 ;
N_DAYS_WIND = 10 ;
N_3H_RAIN = 80 ;
STRING = 8 ;
TIME_Sat = UNLIMITED ; // (1 currently)
variables:
float DATE_MAMMAL(N_prof) ;
DATE_MAMMAL:long_name = "Date of marine mammal profile" ;
DATE_MAMMAL:units = "days since 1990-01-01 00:00:00" ;
DATE_MAMMAL:standard_name = "time" ;
DATE_MAMMAL:FillValue = -999.f ;
```

```

float LATITUDE_MAMMAL(N_prof) ;
LATITUDE_MAMMAL:long_name = "Latitude of marine mammal profile" ;
LATITUDE_MAMMAL:units = "degrees_north" ;
LATITUDE_MAMMAL:valid_min = -90. ;
LATITUDE_MAMMAL:valid_max = 90. ;
LATITUDE_MAMMAL:standard_name = "latitude" ;
LATITUDE_MAMMAL:_FillValue = -999.f ;
float LONGITUDE_MAMMAL(N_prof) ;
LONGITUDE_MAMMAL:long_name = "Longitude of mammal profile" ;
LONGITUDE_MAMMAL:units = "degrees_east" ;
LONGITUDE_MAMMAL:valid_min = -180. ;
LONGITUDE_MAMMAL:valid_max = 180. ;
LONGITUDE_MAMMAL:standard_name = "longitude" ;
LONGITUDE_MAMMAL:_FillValue = -999.f ;
float SSS_DEPTH_MAMMAL(N_prof) ;
SSS_DEPTH_MAMMAL:long_name = "Sea water pressure at marine mammal location (equals
0 at sea level)" ;
SSS_DEPTH_MAMMAL:units = "decibar" ;
SSS_DEPTH_MAMMAL:standard_name = "sea_water_pressure" ;
SSS_DEPTH_MAMMAL:_FillValue = -999.f ;
float SSS_MAMMAL(N_prof) ;
SSS_MAMMAL:long_name = "Mammals SSS" ;
SSS_MAMMAL:units = "1" ;
SSS_MAMMAL:salinity_scale = "Practical Salinity Scale(PSS-78)" ;
SSS_MAMMAL:standard_name = "sea_water_salinity" ;
SSS_MAMMAL:_FillValue = -999.f ;
float SST_MAMMAL(N_prof) ;
SST_MAMMAL:long_name = "Mammals SST" ;
SST_MAMMAL:units = "degree Celsius" ;
SST_MAMMAL:standard_name = "sea_water_temperature" ;
SST_MAMMAL:_FillValue = -999.f ;
float DISTANCE_TO_COAST_MAMMAL(N_prof) ;
DISTANCE_TO_COAST_MAMMAL:long_name = "Distance to coasts at marine mammal loca-
tion" ;
DISTANCE_TO_COAST_MAMMAL:units = "km" ;
DISTANCE_TO_COAST_MAMMAL:_FillValue = -999.f ;
float PLATFORM_NUMBER_MAMMAL(N_prof) ;
PLATFORM_NUMBER_MAMMAL:long_name = "Mammals unique identifier" ;
PLATFORM_NUMBER_MAMMAL:conventions = "WMO float identifier : A9IIII" ;
PLATFORM_NUMBER_MAMMAL:units = "1" ;
PLATFORM_NUMBER_MAMMAL:_FillValue = -999.f ;
float PSAL_MAMMAL(N_prof, N_LEVELS) ;
PSAL_MAMMAL:long_name = "Mammals salinity profile" ;
PSAL_MAMMAL:units = "1" ;
PSAL_MAMMAL:salinity_scale = "Practical Salinity Scale (PSS-78)" ;
PSAL_MAMMAL:standard_name = "sea_water_salinity" ;
PSAL_MAMMAL:_FillValue = -999.f ;
float TEMP_MAMMAL(N_prof, N_LEVELS) ;
TEMP_MAMMAL:long_name = "Mammals temperature profile" ;

```

```

TEMP_MAMMAL:units = "degree Celsius" ;
TEMP_MAMMAL:standard_name = "sea_water_temperature" ;
TEMP_MAMMAL:_FillValue = -999.f ;
float PRES_MAMMAL(N_prof, N_LEVELS) ;
PRES_MAMMAL:long_name = "Mammals pressure profile" ;
PRES_MAMMAL:units = "decibar" ;
PRES_MAMMAL:standard_name = "sea_water_pressure" ;
PRES_MAMMAL:_FillValue = -999.f ;
float RHO_MAMMAL(N_prof, N_LEVELS) ;
RHO_MAMMAL:long_name = "Mammals in-situ density profile" ;
RHO_MAMMAL:units = "kg/m" ;
RHO_MAMMAL:_FillValue = -999.f ;
float SIGMA0_MAMMAL(N_prof, N_LEVELS) ;
SIGMA0_MAMMAL:long_name = "Mammals potential density anomaly profile" ;
SIGMA0_MAMMAL:units = "kg/m3" ;
SIGMA0_MAMMAL:_FillValue = -999.f ;
float N2_MAMMAL(N_prof, N_LEVELS) ;
N2_MAMMAL:long_name = "Mammals buoyancy frequency profile" ;
N2_MAMMAL:units = "1/s2" ;
N2_MAMMAL:_FillValue = -999.f ;
float MLD_MAMMAL(N_prof) ;
MLD_MAMMAL:long_name = "Mixed Layer Depth (MLD) calculated from marine mammal
profile (depth where  $\sigma_0 = \sigma_{010m} + \Delta\sigma_0$  with  $\Delta\sigma_0 = \sigma_0(\theta_{10m} - 0.2, S_{10m}) - \sigma_0(\theta_{10m}, S_{10m})$ )" ;
MLD_MAMMAL:units = "m" ;
MLD_MAMMAL:_FillValue = -999.f ;
float TTD_MAMMAL(N_prof) ;
TTD_MAMMAL:long_name = "Top of Thermocline Depth (TTD) calculated from marine mam-
mal profile (depth where  $\theta = \theta_{10m} - 0.2$ )" ;
TTD_MAMMAL:units = "m" ;
TTD_MAMMAL:_FillValue = -999.f ;
float BLT_MAMMAL(N_prof) ;
BLT_MAMMAL:long_name = "Barrier Layer Thickness (TTD-MLD)" ;
BLT_MAMMAL:units = "m" ;
BLT_MAMMAL:_FillValue = -999.f ;
float DATE_Satellite_product(TIME_Sat) ;
DATE_Satellite_product:long_name = "Central time of satellite SSS file" ;
DATE_Satellite_product:units = "days since 1990-01-01 00:00:00" ;
DATE_Satellite_product:standard_name = "time" ;
float LATITUDE_Satellite_product(N_prof) ;
LATITUDE_Satellite_product:long_name = "Satellite product latitude at marine mammal loca-
tion" ;
LATITUDE_Satellite_product:units = "degrees_north" ;
LATITUDE_Satellite_product:valid_min = -90. ;
LATITUDE_Satellite_product:valid_max = 90. ;
LATITUDE_Satellite_product:standard_name = "latitude" ;
LATITUDE_Satellite_product:_FillValue = -999.f ;
float LONGITUDE_Satellite_product(N_prof) ;
LONGITUDE_Satellite_product:long_name = "Satellite product longitude at marine mammal
location" ;

```

```

LONGITUDE_Satellite_product:units = "degrees_east" ;
LONGITUDE_Satellite_product:valid_min = -180. ;
LONGITUDE_Satellite_product:valid_max = 180. ;
LONGITUDE_Satellite_product:standard_name = "longitude" ;
LONGITUDE_Satellite_product:FillValue = -999.f ;
float SSS_Satellite_product(N_prof) ;
SSS_Satellite_product:long_name = "Satellite product SSS at marine mammal location" ;
SSS_Satellite_product:units = "1" ;
SSS_Satellite_product:salinity_scale = "Practical Salinity Scale(PSS-78)" ;
SSS_Satellite_product:standard_name = "sea_surface_salinity" ;
SSS_Satellite_product:FillValue = -999.f ;
float SST_Satellite_product(N_prof) ;
SST_Satellite_product:long_name = "Satellite product SST at marine mammal location" ;
SST_Satellite_product:units = "degree Celsius" ;
SST_Satellite_product:standard_name = "sea_surface_temperature" ;
SST_Satellite_product:FillValue = -999.f ;
float Spatial_lags(N_prof) ;
Spatial_lags:long_name = "Spatial lag between marine mammal location and satellite SSS product pixel center" ;
Spatial_lags:units = "km" ;
Spatial_lags:FillValue = -999.f ;
float Time_lags(N_prof) ;
Time_lags:long_name = "Temporal lag between marine mammal time and satellite SSS product central time" ;
Time_lags:units = "days" ;
Time_lags:FillValue = -999.f ;
float ROSSBY_RADIUS_at_MAMMAL(N_prof) ;
ROSSBY_RADIUS_at_MAMMAL:long_name = "Baroclinic Rossby radius of deformation (Chelton et al., 1998) at marine mammal location" ;
ROSSBY_RADIUS_at_MAMMAL:units = "km" ;
ROSSBY_RADIUS_at_MAMMAL:FillValue = -999.f ;
float Ascet_daily_wind_at_MAMMAL(N_prof) ;
Ascet_daily_wind_at_MAMMAL:long_name = "Daily Ascet wind speed module at marine mammal location" ;
Ascet_daily_wind_at_MAMMAL:units = "m/s" ;
Ascet_daily_wind_at_MAMMAL:FillValue = -999.f ;
float CMORPH_3h_Rain_Rate_at_MAMMAL(N_prof) ;
CMORPH_3h_Rain_Rate_at_MAMMAL:long_name = "3-hourly CMORPH rain rate at marine mammal location" ;
CMORPH_3h_Rain_Rate_at_MAMMAL:units = "mm/3h" ;
CMORPH_3h_Rain_Rate_at_MAMMAL:FillValue = -999.f ;
float Ascet_10_prior_days_wind_at_MAMMAL(N_prof, N_DAYS_WIND) ;
Ascet_10_prior_days_wind_at_MAMMAL:long_name = "Prior 10 days time series of Ascet wind speed module at marine mammal location" ;
Ascet_10_prior_days_wind_at_MAMMAL:units = "m/s" ;
Ascet_10_prior_days_wind_at_MAMMAL:FillValue = -999.f ;
float CMORPH_10_prior_days_Rain_Rate_at_MAMMAL(N_prof, N_3H_RAIN) ;
CMORPH_10_prior_days_Rain_Rate_at_MAMMAL:long_name = "Prior 10 days times series of 3-hourly CMORPH Rain Rate at marine mammal location" ;

```

```

CMORPH_10_prior_days_Rain_Rate_at_MAMMAL:units = "mm/3h" ;
CMORPH_10_prior_days_Rain_Rate_at_MAMMAL:FillValue = -999.f ;
float SSS_ISAS_at_MAMMAL(N_prof) ;
SSS_ISAS_at_MAMMAL:long_name = "ISAS SSS (5m depth) at marine mammal location" ;
SSS_ISAS_at_MAMMAL:units = "1" ;
SSS_ISAS_at_MAMMAL:salinity_scale = "Practical Salinity Scale(PSS-78)" ;
SSS_ISAS_at_MAMMAL:standard_name = "sea_water_salinity" ;
SSS_ISAS_at_MAMMAL:FillValue = -999.f ;
float SSS_PCTVAR_ISAS_at_MAMMAL(N_prof) ;
SSS_PCTVAR_ISAS_at_MAMMAL:long_name = "Error on ISAS SSS (5m depth) at marine
mammal location (% variance)" ;
SSS_PCTVAR_ISAS_at_MAMMAL:units = "%" ;
SSS_PCTVAR_ISAS_at_MAMMAL:FillValue = -999.f ;
float SSS_WOA13_at_MAMMAL(N_prof) ;
SSS_WOA13_at_MAMMAL:long_name = "WOA 2013 (DECAV-1deg) SSS (0m depth) at marine
mammal location" ;
SSS_WOA13_at_MAMMAL:units = "1" ;
SSS_WOA13_at_MAMMAL:salinity_scale = "Practical Salinity Scale(PSS-78)" ;
SSS_WOA13_at_MAMMAL:standard_name = "sea_surface_salinity" ;
SSS_WOA13_at_MAMMAL:FillValue = -999.f ;
float SSS_STD_WOA13_at_MAMMAL(N_prof) ;
SSS_STD_WOA13_at_MAMMAL:long_name = "WOA 2013 (DECAV-1deg) SSS STD (0m depth)
at marine mammal location " ;
SSS_STD_WOA13_at_MAMMAL:units = "1" ;
SSS_STD_WOA13_at_MAMMAL:FillValue = -999.f ;

```

```

// global attributes:
:Conventions = "CF-1.6" ;
:title = "Marine Mammals Match-Up Database" ; :Satellite_product_name = "SMOS L3 CATDS
CECOS LOCEAN V2.1 9DAYS 25KM" ;
:Satellite_product_spatial_resolution = "25 km" ;
:Satellite_product_temporal_resolution = "9 days" ;
:Satellite_product_filename = "v2.1/9days/SMOS.L3-DEBIAS-LOCEAN-AD-20100116-EASE-09d.25km-v00.nc"
;
:Match-Up_spatial_window_radius_in_km = 25. ;
:Match-Up_temporal_window_radius_in_days = 2. ;
:start_time = "20100114T000005Z" ;
:stop_time = "20100118T235026Z" ;
:northernmost_latitude = 77.676f ;
:southernmost_latitude = -66.423f ;
:westernmost_longitude = -179.219f ;
:easternmost_longitude = 179.199f ;
:geospatial_lat_units = "degrees north" ;
:geospatial_lat_resolution = "25 km" ;
:geospatial_lon_units = "degrees east" ;
:geospatial_lon_resolution = "25 km" ;
:institution = "ESA-IFREMER-ODL" ;
:project_name = "SMOS Pilote Mission Exploitation Platfrom (Pi-MEP) for salinity" ;
:project_url = "https://pimep-project.odl.bzh" ;

```

```

:license = "Pi-MEP data use is free and open" ;
:product_version = "1.0" ;
:keywords = "Oceans > Ocean Salinity > Sea Surface Salinity" ;
:acknowledgment = "Please acknowledge the use of these data with the following statement:
These data were provided by SMOS Pilote Mission Exploitation Platfrom (Pi-MEP) for salin-
ity" ;
:source = "v2.1/9days/SMOS_L3_DEBIAS_LOCEAN_AD_20100116_EASE_09d_25km_v00.nc" ;
:references = "https://pimep-project.odl.bzh" ;
:history = "Processed on 2018-04-18 using MDB-generator" ;
:date_created = "2018-04-18 17:09:30" ;
}

```

2.5 MDB characteristics for the particular in situ/satellite pairs

2.5.1 Number of paired SSS data as a function of time and distance to coast

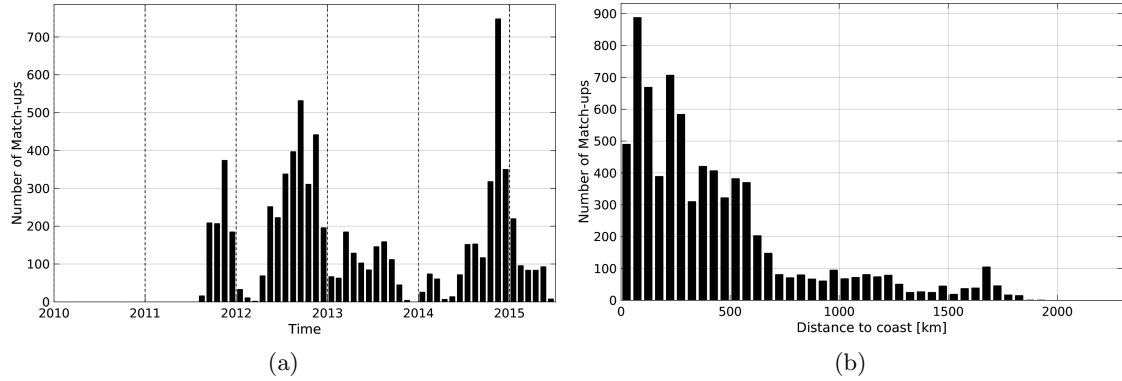


Figure 1: Number of match-ups between Sea mammals and Aquarius-L3-JPL-V4-7DAY-RUNNING SSS as a function of time (a) and as function of the distance to coast (b) over the Indian Ocean Pi-MEP region and for the full satellite product period.

2.5.2 Histograms of the SSS match-ups

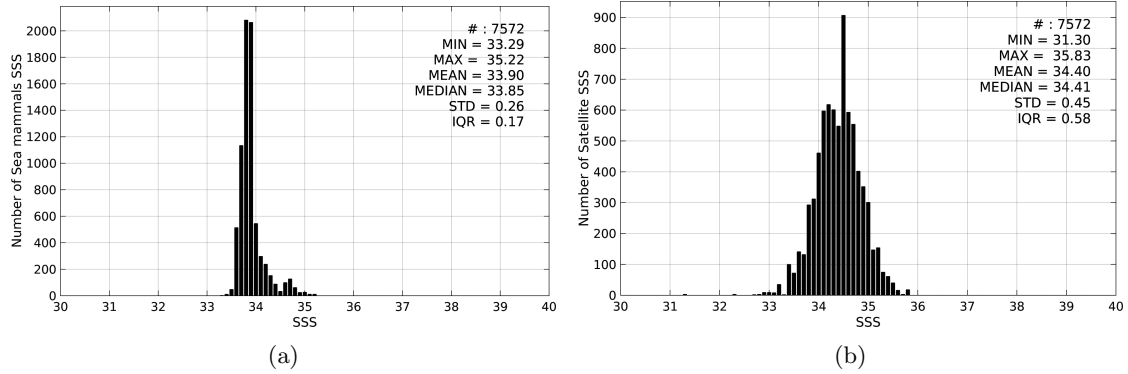


Figure 2: Histograms of SSS from Sea mammals (a) and Aquarius-L3-JPL-V4-7DAY-RUNNING (b) considering all match-up pairs per bins of 0.1 over the Indian Ocean Pi-MEP region and for the full satellite product period.

2.5.3 Distribution in situ SSS depth in match-ups pairs

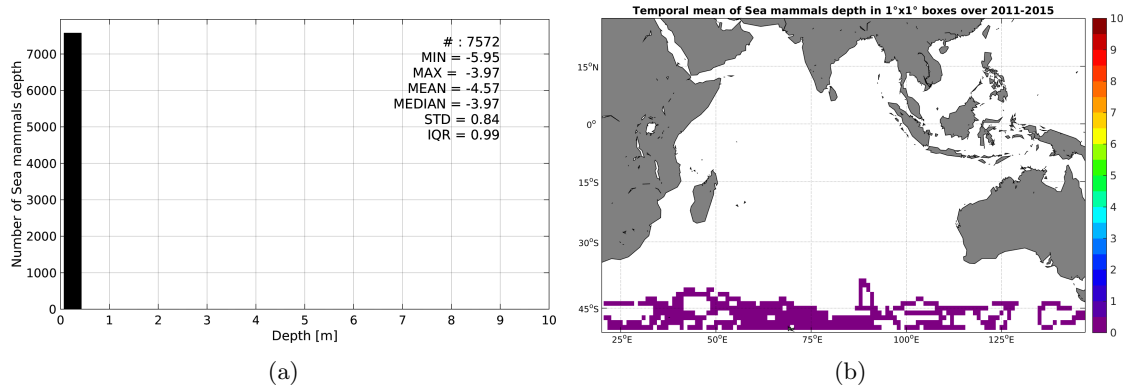


Figure 3: Histograms of the depth of the upper level SSS measurements from Sea mammals in the Match-up DataBase for the Indian Ocean Pi-MEP region (a) and temporal mean spatial distribution of pressure of the in situ SSS data over 1°x1° boxes and for the full satellite product period (b).

2.5.4 Spatial Distribution of Match-ups

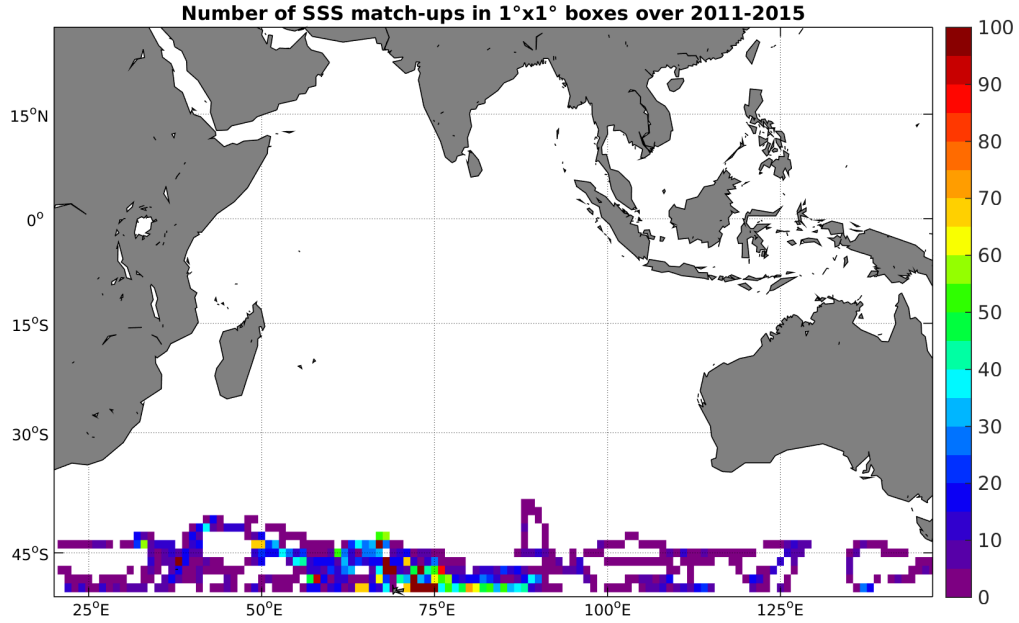


Figure 4: Number of SSS match-ups between Sea mammals SSS and the Aquarius-L3-JPL-V4-7DAY-RUNNING SSS product for the Indian Ocean Pi-MEP region over $1^\circ \times 1^\circ$ boxes and for the full satellite product period.

2.5.5 Histograms of the spatial and temporal lags of the match-up pairs

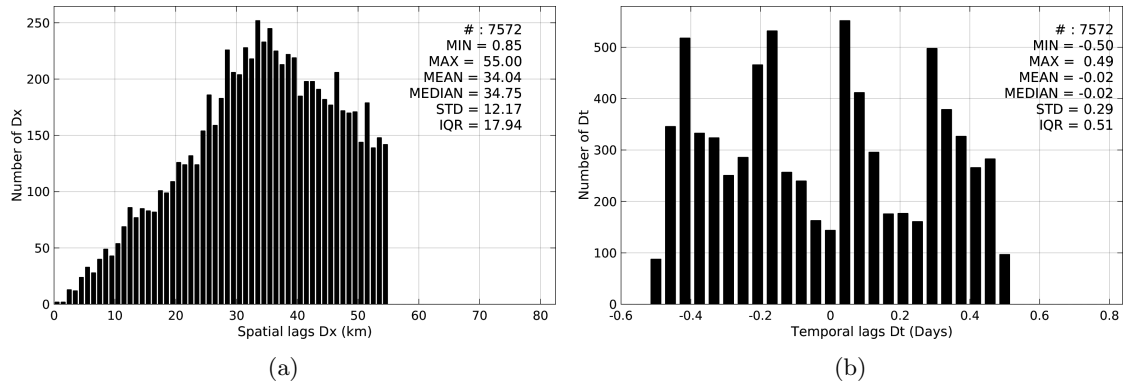


Figure 5: Histograms of the spatial (a) and temporal (b) lags between the time of the Sea mammals measurements and the date of the corresponding Aquarius-L3-JPL-V4-7DAY-RUNNING SSS product.

3 MDB file Analyses

3.1 Spatial Maps of the Temporal mean and STD of in situ and satellite SSS and of the difference (Δ SSS)

In Figure 6, we show maps of temporal mean (left) and standard deviation (right) of the Aquarius-L3-JPL-V4-7DAY-RUNNING satellite SSS product (top) and of the Sea mammals in situ dataset at the collected Pi-MEP match-up pairs. The temporal mean and std are gridded over the full satellite product period and over spatial boxes of size $1^\circ \times 1^\circ$.

At the bottom of Figure 6, the temporal mean (left) and standard deviation (right) of the differences between the satellite SSS product and in situ data found at match-up pairs, namely Δ SSS(Satellite -Sea mammals), is also gridded over the full satellite product period and over spatial boxes of size $1^\circ \times 1^\circ$.

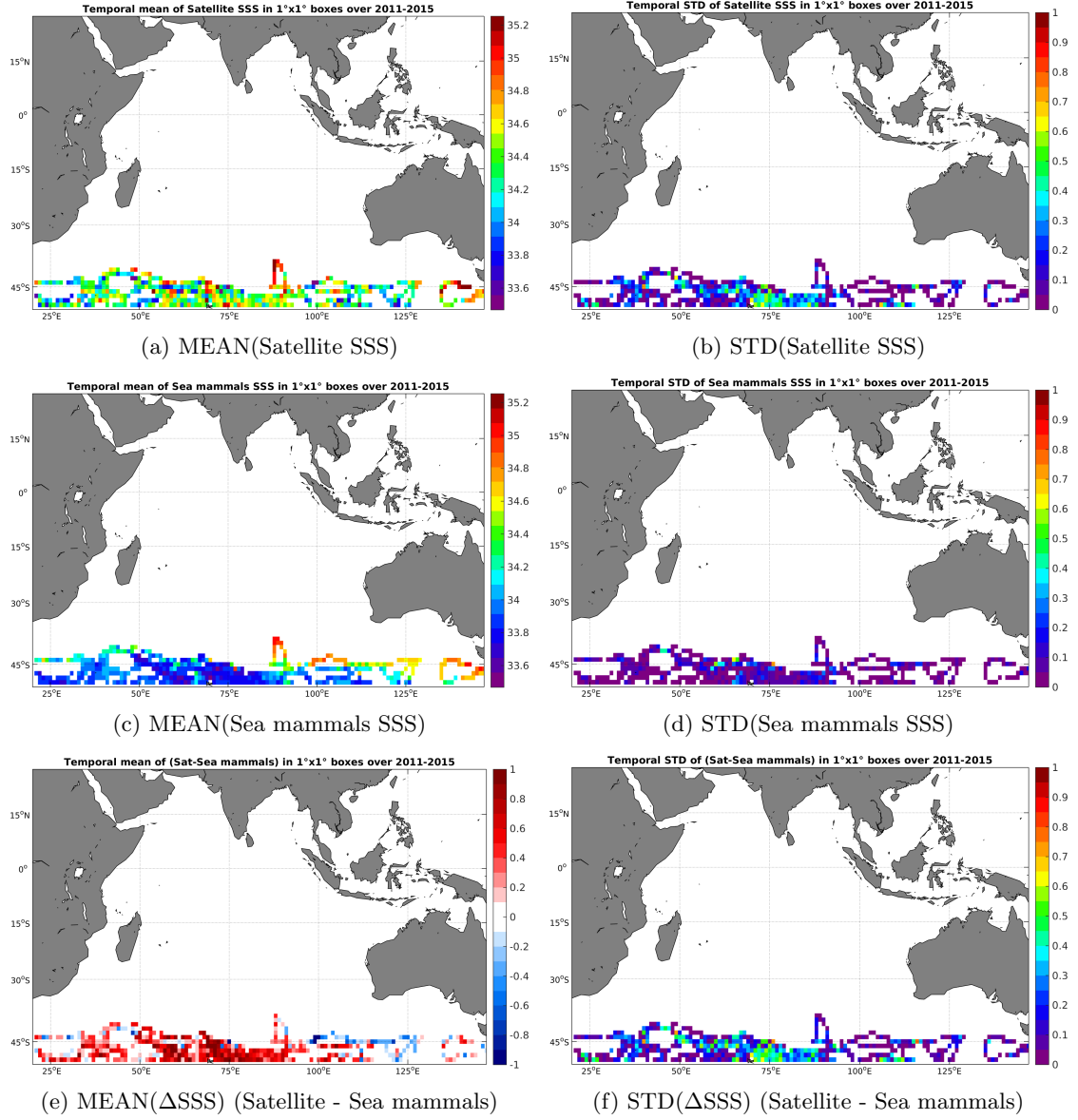


Figure 6: Temporal mean (left) and STD (right) of SSS from Aquarius-L3-JPL-V4-7DAY-RUNNING (top), Sea mammals (middle), and of Δ SSS (Satellite - Sea mammals). Only match-up pairs are used to generate these maps.

3.2 Time series of the monthly averaged mean and STD of in situ and satellite SSS and of the (Δ SSS)

In the top panel of Figure 7, we show the time series of the monthly averaged SSS estimated over the full Indian Ocean Pi-MEP region for both Aquarius-L3-JPL-V4-7DAY-RUNNING satellite SSS product (in black) and the Sea mammals in situ dataset (in blue) at the collected Pi-MEP match-up pairs.

In the middle panel of Figure 7, we show the time series of the monthly averaged Δ SSS

(Satellite - Sea mammals) for the collected Pi-MEP match-up pairs and estimated over the full Indian Ocean Pi-MEP region.

In the bottom panel of Figure 7, we show the time series of the monthly averaged standard deviation of the ΔSSS (Satellite - Sea mammals) for the collected Pi-MEP match-up pairs and estimated over the full Indian Ocean Pi-MEP region.

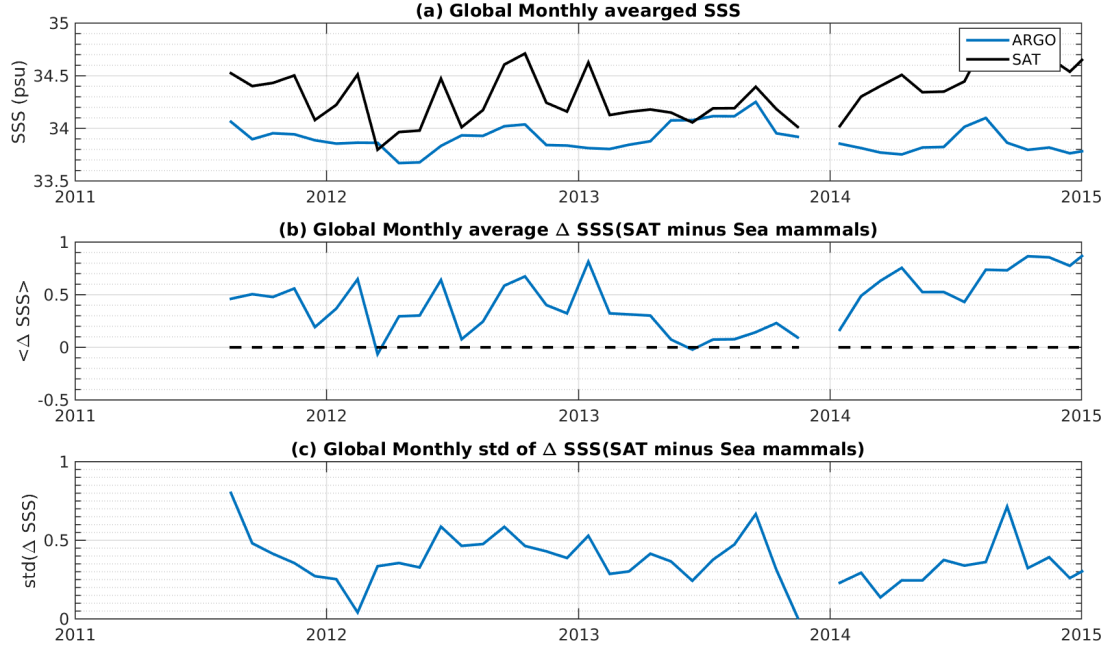


Figure 7: Time series of the monthly averaged mean SSS (top), mean ΔSSS (Satellite - Sea mammals) and STD of ΔSSS (Satellite - Sea mammals) over the Indian Ocean Pi-MEP region considering all match-ups collected by the Pi-MEP platform.

3.3 Zonally-averaged Time-mean and temporal STD of in situ and satellite SSS and of the ΔSSS

In Figure 8 left panel, we show the zonally averaged time-mean SSS estimated at the collected Pi-MEP match-up pairs for both Aquarius-L3-JPL-V4-7DAY-RUNNING satellite SSS product (in black) and the Sea mammals in situ dataset (in blue). The time mean is evaluated over the full satellite SSS product period.

In the right panel of Figure 8, we show the zonally averaged time-mean ΔSSS (Satellite - Sea mammals) for all the collected Pi-MEP match-up pairs estimated over the full satellite product period.

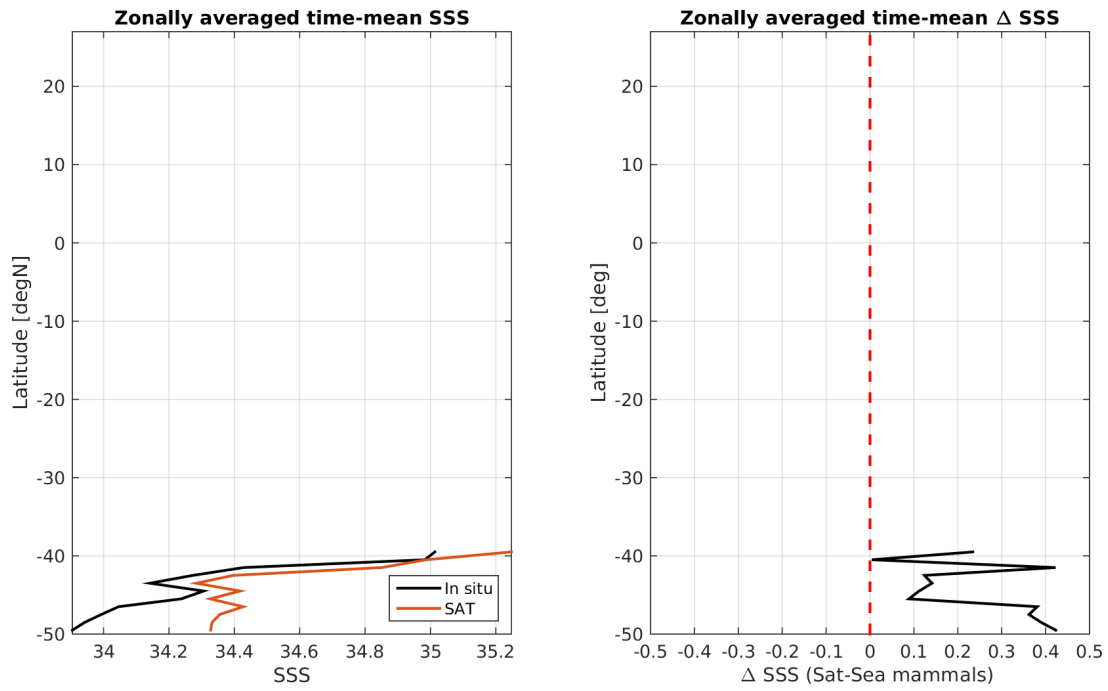


Figure 8: Left panel: Zonally averaged time mean SSS from Aquarius-L3-JPL-V4-7DAY-RUNNING (black) and from Sea mammals (blue). Right panel: zonally averaged time-mean Δ SSS (Satellite - Sea mammals) for all the collected Pi-MEP match-up pairs estimated over the full satellite product period.

3.4 Scatterplots of satellite vs in situ SSS by latitudinal bands

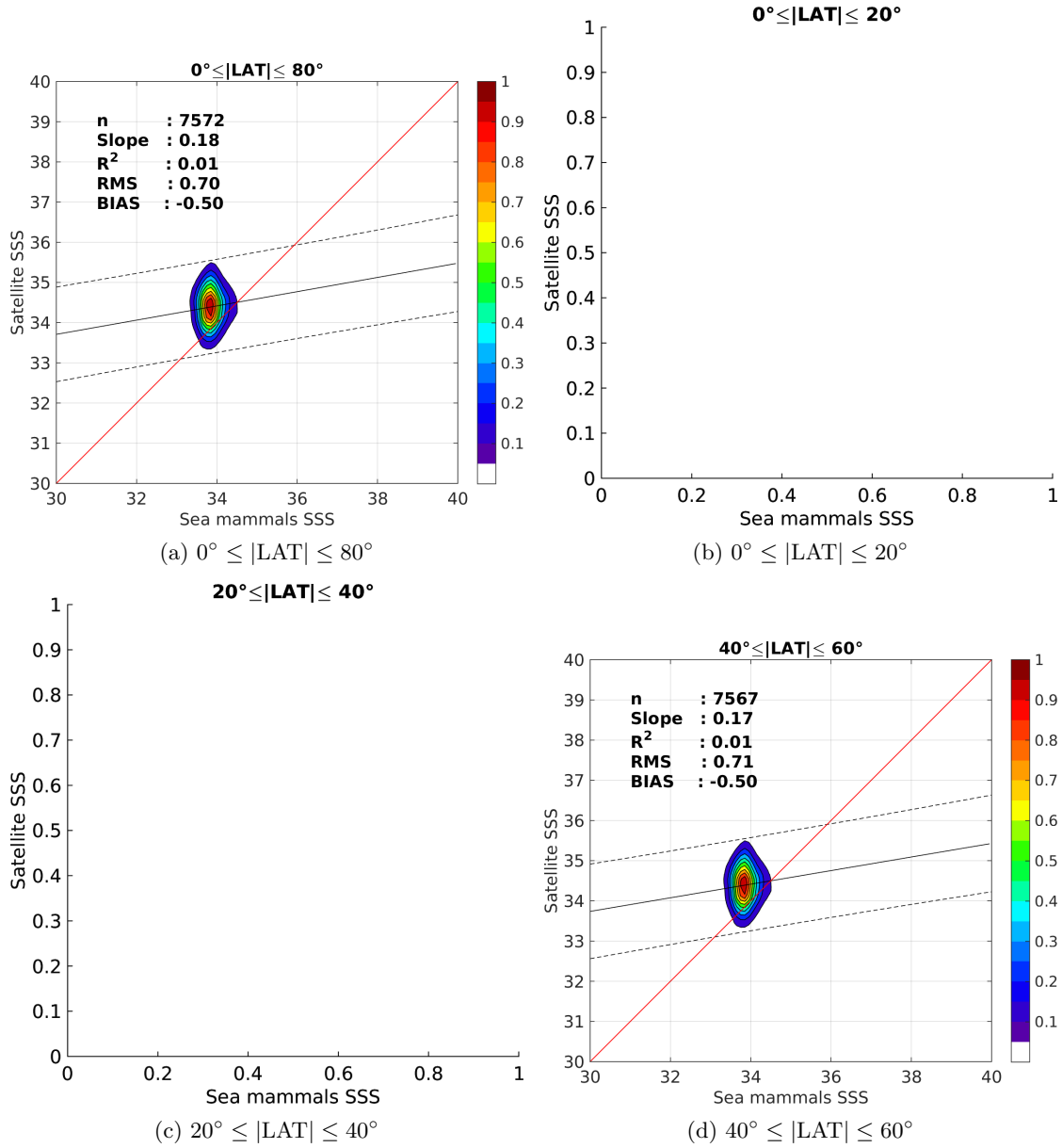


Figure 9: Contour maps of the concentration of Aquarius-L3-JPL-V4-7DAY-RUNNING SSS (y-axis) versus Sea mammals SSS (x-axis) at match-up pairs for different latitude bands. For each plot, the red line shows $x=y$. The black thin and dashed lines indicate a linear fit through the data cloud and the $\pm 95\%$ confidence levels, respectively. The number match-up pairs n , the slope and R^2 coefficient of the linear fit, the root mean square (RMS) and the mean bias between satellite and in situ data are indicated for each latitude band in each plots.

3.5 Time series of the monthly averaged mean and STD of the ΔSSS sorted by latitudinal bands

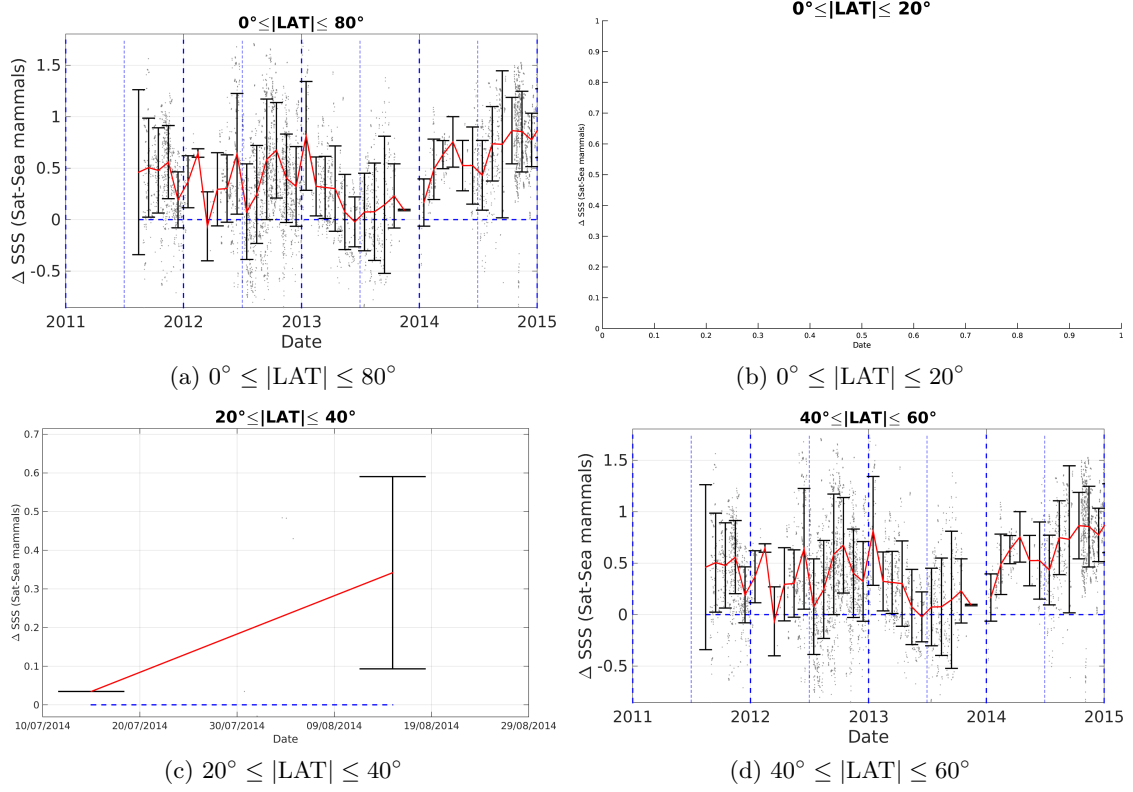


Figure 10: Monthly-average mean (red curves) ΔSSS (Satellite - Sea mammals) and ± 1 STD (black vertical thick bars) as function of time for all the collected Pi-MEP match-up pairs estimated over the Indian Ocean Pi-MEP region and for the full satellite product period are shown for different latitude bands: (a) Latitude band $80^\circ S - 80^\circ N$, (b) latitude band $20^\circ S - 20^\circ N$, (c) Mid Latitude bands $40^\circ S - 20^\circ S$ and $20^\circ N - 40^\circ N$ and (d) Latitude bands $60^\circ S - 40^\circ S$ and $40^\circ N - 60^\circ N$.

3.6 ΔSSS sorted as function of geophysical conditions

In Figure 11, we classify the match-up differences ΔSSS (Satellite - in situ) between Aquarius-L3-JPL-V4-7DAY-RUNNING and Sea mammals SSS as function of the geophysical conditions at match-up points. The mean and std of ΔSSS (Satellite - Sea mammals) is thus evaluated as function of the

- in situ SSS values per bins of width 0.2,
- in situ SST values per bins of width $1^\circ C$,
- ASCAT daily wind values per bins of width 1 m/s,
- CMORPH 3-hourly rain rates per bins of width 1 mm/h, and,
- distance to coasts per bins of width 50 km.

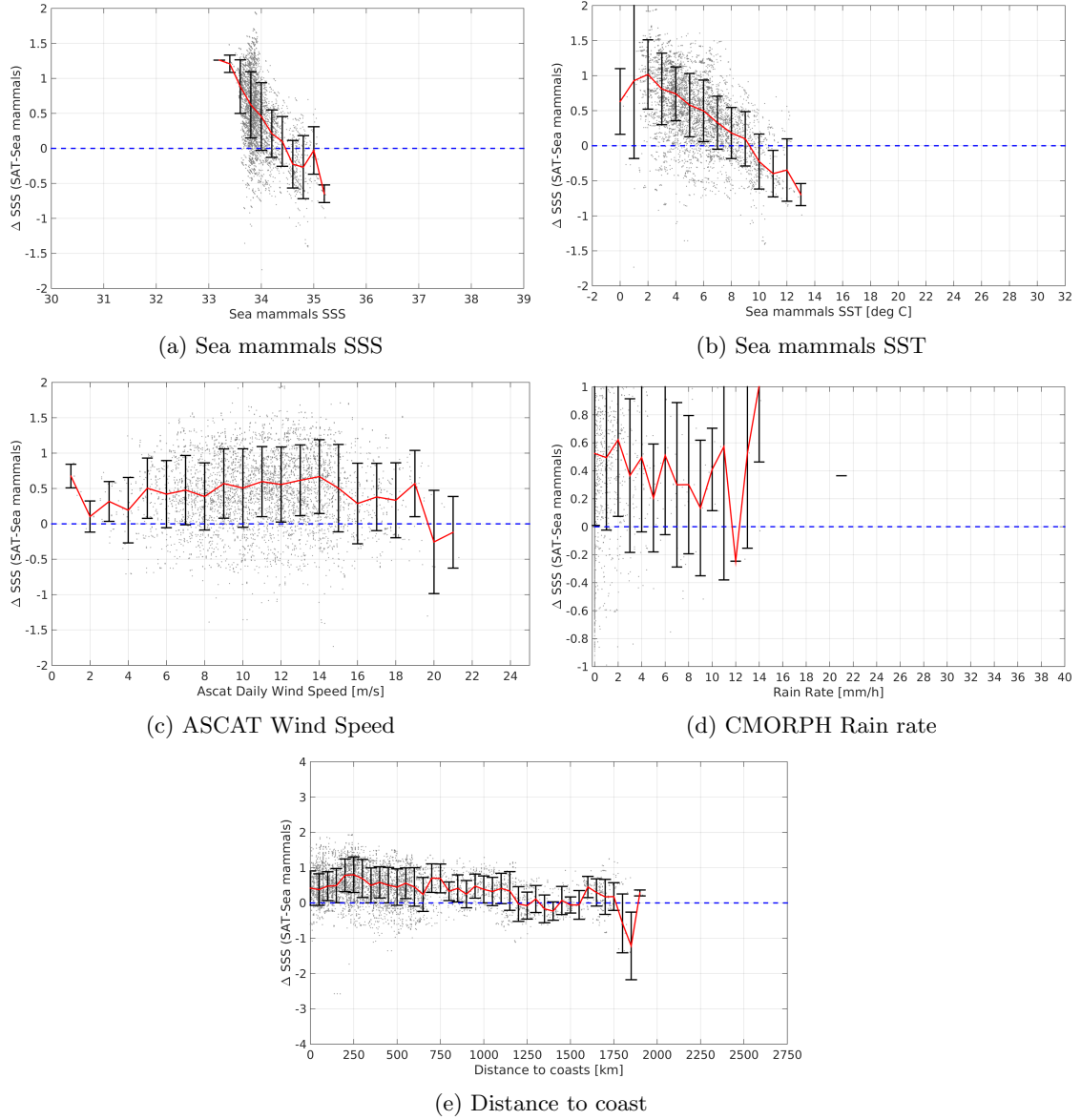


Figure 11: ΔSSS (Satellite - Sea mammals) sorted as function of Sea mammals SSS values a), Sea mammals SST b), ASCAT Wind speed c), CMORPH rain rate d) and distance to coast (e). In all plots the mean and STD of ΔSSS for each bin is indicated by the red curves and black vertical thick bars (± 1 STD)

In Figures 12 and 13, we focus on sub-datasets of the match-up differences ΔSSS (Satellite - in situ) between Aquarius-L3-JPL-V4-7DAY-RUNNING and Sea mammals for the following specific geophysical conditions:

- **C1**:if the local value at in situ location of estimated rain rate is high (ie. > 10 mm/h) and mean daily wind is low (ie. < 5 m/s).
- **C2**:if the prior 10-days history of the rain and wind at in situ location show high (ie. > 5

mm/h) and low (ie. < 5 m/s) median values, respectively.

- **C3**:if both C1 and C2 are met.
- **C4**:if the mixed layer is shallow with depth < 20 m.
- **C5**:if there is a barrier layer with thickness > 10 m.
- **C6**:if the in situ data is located where the climatological sss standard deviation is high (ie. above > 0.2).

For each of these conditions, the temporal mean (gridded over spatial boxes of size $1^\circ \times 1^\circ$) and the histogram of the difference ΔSSS (Satellite - in situ) are presented.

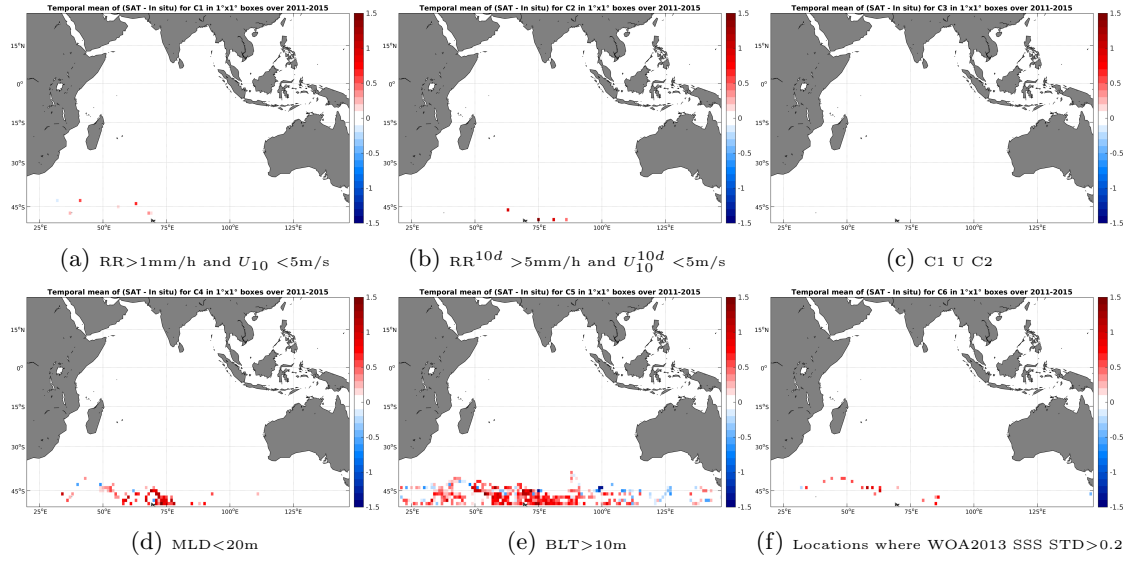


Figure 12: Temporal mean gridded over spatial boxes of size $1^\circ \times 1^\circ$ of ΔSSS (Aquarius-L3-JPL-V4-7DAY-RUNNING - Sea mammals) for 6 different subdatasets corresponding to: $RR > 1\text{mm/h}$ and $U_{10} < 5\text{m/s}$ (a), $RR^{10d} > 5\text{mm/h}$ and $U_{10}^{10d} < 5\text{m/s}$ (b), C1 U C2 (c), $MLD < 20\text{m}$ (d), $BLT > 10\text{m}$ (e), Locations where WOA2013 SSS STD > 0.2 (f).

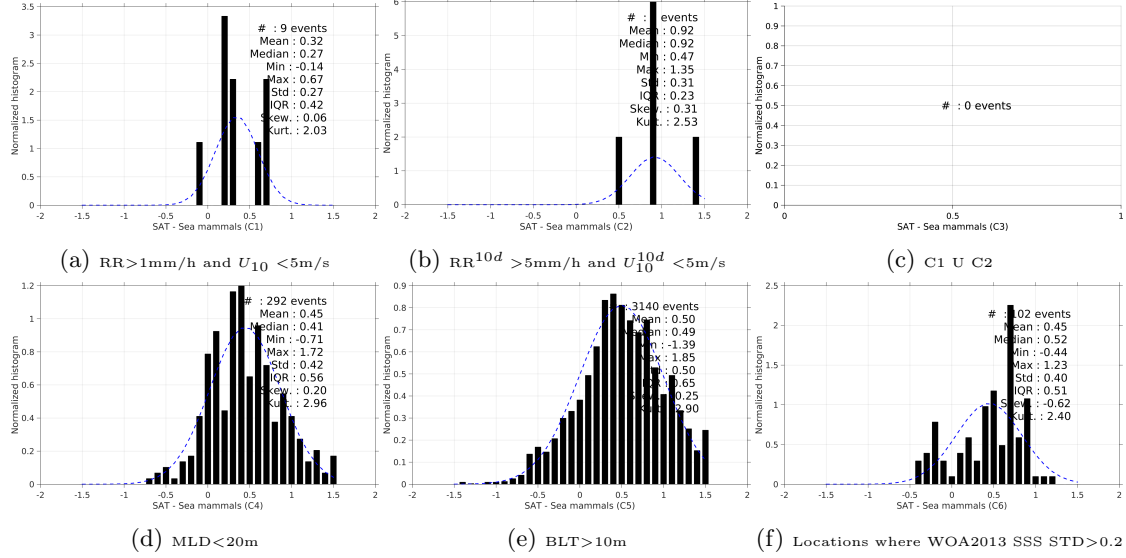


Figure 13: Normalized histogram of ΔSSS (Aquarius-L3-JPL-V4-7DAY-RUNNING - Sea mammals) for 6 different subdatasets corresponding to: $RR > 1\text{mm/h}$ and $U_{10} < 5\text{m/s}$ (a), $RR^{10d} > 5\text{mm/h}$ and $U_{10}^{10d} < 5\text{m/s}$ (b), C1 U C2 (c), $MLD < 20\text{m}$ (d), $BLT > 10\text{m}$ (e), Locations where WOA2013 SSS STD > 0.2 (f).

4 Summary

Table 1 presents statistics (mean, median, standard deviation, root mean square and inter-quantile range) of the match-up differences ΔSSS (Satellite - in situ) between Aquarius-L3-JPL-V4-7DAY-RUNNING and Sea mammals derived over the Indian Ocean Pi-MEP region and for the full satellite product period and for the following conditions:

- all: All the match-up pairs satellite/in situ SSS are used to derive the statistics
- C1: only pairs where $RR > 1\text{mm/h}$ and $U_{10} < 5\text{m/s}$
- C2: only pairs where $RR^{10d} > 5\text{mm/h}$ and $U_{10}^{10d} < 5\text{m/s}$
- C3: only pairs where C1 U C2
- C4: only pairs where $MLD < 20\text{m}$
- C5: only pairs where $BLT > 10\text{m}$
- C6: only pairs at Locations where WOA2013 SSS STD > 0.2
- C7a: only pairs where distance to coast is $< 150\text{ km}$.
- C7b: only pairs where distance to coast is in the range $[150, 800]\text{ km}$.
- C7c: only pairs where distance to coast is $> 800\text{ km}$.
- C8a: only pairs where in situ SST is $< 5^\circ\text{C}$.
- C8b: only pairs where in situ SST is in the range $[5, 28]^\circ\text{C}$.

- C8c: only pairs where in situ SST is $> 28^{\circ}\text{C}$.
- C9a: only pairs where in situ SSS is < 33 .
- C9b: only pairs where in situ SSS is in the range $[33, 37]$.
- C9c: only pairs where in situ SSS is > 37 .

Table 1: Statistics of ΔSSS (Satellite - Sea mammals)

Condition	#	Median	Mean	Std	RMS	IQR
all	7572	0.49	0.50	0.50	0.70	0.66
C1	9	0.27	0.32	0.27	0.41	0.42
C2	5	0.92	0.92	0.31	0.96	0.23
C3	0	NaN	NaN	NaN	NaN	NaN
C4	292	0.41	0.45	0.42	0.62	0.56
C5	3140	0.49	0.50	0.50	0.71	0.65
C6	102	0.52	0.45	0.40	0.60	0.51
C7a	2047	0.44	0.49	0.44	0.66	0.55
C7b	4395	0.61	0.58	0.51	0.77	0.68
C7c	1130	0.25	0.22	0.45	0.50	0.61
C8a	3789	0.74	0.70	0.47	0.85	0.61
C8b	3783	0.31	0.30	0.43	0.53	0.55
C8c	0	NaN	NaN	NaN	NaN	NaN
C9a	0	NaN	NaN	NaN	NaN	NaN
C9b	7572	0.49	0.50	0.50	0.70	0.66
C9c	0	NaN	NaN	NaN	NaN	NaN

For the same conditions, Table 2 presents statistics of ΔSSS (Satellite - ISAS). Only ISAS SSS values with $\text{PCTVAR} < 80\%$ are used to derive the statistics.

Table 2: Statistics of ΔSSS (Satellite - ISAS)

Condition	#	Median	Mean	Std	RMS	IQR
all	7572	0.50	0.49	0.50	0.70	0.64
C1	9	0.32	0.24	0.29	0.36	0.23
C2	5	0.84	0.92	0.29	0.96	0.26
C3	0	NaN	NaN	NaN	NaN	NaN
C4	292	0.43	0.47	0.39	0.61	0.47
C5	3140	0.48	0.48	0.50	0.69	0.63
C6	102	0.35	0.37	0.36	0.52	0.42
C7a	1754	0.48	0.51	0.43	0.67	0.54
C7b	4329	0.59	0.56	0.51	0.76	0.67
C7c	1113	0.22	0.21	0.43	0.47	0.54
C8a	3679	0.70	0.70	0.47	0.84	0.60
C8b	3517	0.28	0.28	0.43	0.51	0.54
C8c	0	NaN	NaN	NaN	NaN	NaN
C9a	0	NaN	NaN	NaN	NaN	NaN
C9b	7196	0.50	0.49	0.49	0.70	0.64
C9c	0	NaN	NaN	NaN	NaN	NaN

References

- Abderrahim Bentamy and Denis Croize Fillon. Gridded surface wind fields from Metop/ASCAT measurements. *Int. J. Remote Sens.*, 33(6):1729–1754, March 2012. ISSN 1366-5901. doi: [10.1080/01431161.2011.600348](https://doi.org/10.1080/01431161.2011.600348).
- Abderrahim Bentamy, Semyon A. Grodsky, James A. Carton, Denis Croizé-Fillon, and Bertrand Chapron. Matching ASCAT and QuikSCAT winds. *J. Geophys. Res.*, 117(C2), February 2012. ISSN 0148-0227. doi: [10.1029/2011JC007479](https://doi.org/10.1029/2011JC007479). C02011.
- Jaqueline Boutin, Y. Chao, W. E. Asher, T. Delcroix, R. Drucker, K. Drushka, N. Kolodziejczyk, T. Lee, N. Reul, G. Reverdin, J. Schanze, A. Soloviev, L. Yu, J. Anderson, L. Brucker, E. Dinnat, A. S. Garcia, W. L. Jones, C. Maes, T. Meissner, W. Tang, N. Vinogradova, and B. Ward. Satellite and In Situ Salinity: Understanding Near-Surface Stratification and Sub-footprint Variability. *Bull. Am. Meteorol. Soc.*, 97(8):1391–1407, 2016. ISSN 1520-0477. doi: [10.1175/bams-d-15-00032.1](https://doi.org/10.1175/bams-d-15-00032.1).
- Clément de Boyer Montégut, Gurvan Madec, A. S. Fischer, A. Lazar, and D. Ludicone. Mixed layer depth over the global ocean: An examination of profile data and a profile-based climatology. *J. Geophys. Res.*, 109(C12):C12003, December 2004. ISSN 0148-0227. doi: [10.1029/2004jc002378](https://doi.org/10.1029/2004jc002378).
- Clément de Boyer Montégut, Juliette Mignot, Alban Lazar, and Sophie Cravatte. Control of salinity on the mixed layer depth in the world ocean: 1. General description. *J. Geophys. Res.*, 112(C6):C06011, June 2007. ISSN 0148-0227. doi: [10.1029/2006jc003953](https://doi.org/10.1029/2006jc003953).
- Ralph R. Ferraro. Ssm/i derived global rainfall estimates for climatological applications. *J. Geophys. Res.*, 1021:16715–16736, 07 1997. doi: [10.1029/97JD01210](https://doi.org/10.1029/97JD01210).
- Ralph R. Ferraro, Fuzhong Weng, Norman C. Grody, and Limin Zhao. Precipitation characteristics over land from the NOAA-15 AMSU sensor. *Geophys. Res. Lett.*, 27(17):2669–2672, 2000. doi: [10.1029/2000GL011665](https://doi.org/10.1029/2000GL011665).
- Fabienne Gaillard, E. Autret, V. Thierry, P. Galaup, C. Coatanoan, and T. Loubrieu. Quality Control of Large Argo Datasets. *J. Atmos. Oceanic Technol.*, 26(2):337–351, 2012/10/10 2009. doi: [10.1175/2008JTECHO552.1](https://doi.org/10.1175/2008JTECHO552.1).
- Fabienne Gaillard, Thierry Reynaud, Virginie Thierry, Nicolas Kolodziejczyk, and Karina von Schuckmann. In Situ-Based Reanalysis of the Global Ocean Temperature and Salinity with ISAS: Variability of the Heat Content and Steric Height. *J. Clim.*, 29(4):1305–1323, February 2016. ISSN 1520-0442. doi: [10.1175/jcli-d-15-0028.1](https://doi.org/10.1175/jcli-d-15-0028.1).
- Robert J. Joyce, John E. Janowiak, Phillip A. Arkin, and Pingping Xie. CMORPH: A Method that Produces Global Precipitation Estimates from Passive Microwave and Infrared Data at High Spatial and Temporal Resolution. *J. Hydrometeorol.*, 5(3):487–503, June 2004. ISSN 1525-7541. doi: [10.1175/1525-7541\(2004\)005<0487:camtpg>2.0.co;2](https://doi.org/10.1175/1525-7541(2004)005<0487:camtpg>2.0.co;2).
- Nicolas Kolodziejczyk, Gilles Reverdin, and Alban Lazar. Interannual Variability of the Mixed Layer Winter Convection and Spice Injection in the Eastern Subtropical North Atlantic. *J. Phys. Oceanogr.*, 45(2):504–525, Feb 2015. ISSN 1520-0485. doi: [10.1175/jpo-d-14-0042.1](https://doi.org/10.1175/jpo-d-14-0042.1).
- Christian Kummerow, Y. Hong, W. S. Olson, S. Yang, R. F. Adler, J. McCollum, R. Ferraro, G. Petty, D-B. Shin, and T. T. Wilheit. The Evolution of the Goddard Profiling Algorithm

(GPROF) for Rainfall Estimation from Passive Microwave Sensors. *J. Appl. Meteorol.*, 40(11): 1801–1820, 2001. doi: [10.1175/1520-0450\(2001\)040<1801:TEOTGP>2.0.CO;2](https://doi.org/10.1175/1520-0450(2001)040<1801:TEOTGP>2.0.CO;2).

Anne Treasure, Fabien Roquet, Isabelle Ansorge, Marthán Bester, Lars Boehme, Horst Bornemann, Jean-Benoît Charrassin, Damien Chevallier, Daniel Costa, Mike Fedak, Christophe Guinet, Mike Hammill, Robert Harcourt, Mark Hindell, Kit Kovacs, Mary-Anne Lea, Phil Lovell, Andrew Lowther, Christian Lydersen, Trevor McIntyre, Clive McMahon, Mônica Muelbert, Keith Nicholls, Baptiste Picard, Gilles Reverdin, Andrew Trites, Guy Williams, and P.J. Nico de Bruyn. Marine Mammals Exploring the Oceans Pole to Pole: A Review of the MEOP Consortium. *Oceanography*, 30(2):132–138, jun 2017. doi: [10.5670/oceanog.2017.234](https://doi.org/10.5670/oceanog.2017.234).